



# A generalized framework for designing open-source natural hazard parametric insurance

Carmen B. Steinmann<sup>1,2</sup> · Benoît P. Guillod<sup>3</sup> · Christopher Fairless<sup>3</sup> · David N. Bresch<sup>1,2</sup>

Accepted: 5 August 2023 / Published online: 2 September 2023  
© The Author(s) 2023

## Abstract

Parametric insurance schemes allow for payouts to be triggered by real-time hydro-/meteorological parameters instead of waiting for damage assessments, which means they can be settled swiftly, giving people access to funds right after the event. In this work we propose a framework to design parametric insurance schemes and systematically quantify the basis risk: the difference between the parameter-based payout and the actual damage. We implement the framework in the open-source global risk assessment platform CLIMADA and illustrate it with two stylized parametric insurance case studies, targeting tropical cyclones in Mozambique and winter storms in France. The data used and the provided code base are globally-consistent, open-source, and readily available. The presented methods are therefore applicable in data-scarce areas and accessible to stakeholders from the public and private sector. Moreover, our approach can easily be adapted to other hazards and exposures worldwide. This improves the accessibility and transparency of such innovative insurance schemes.

**Keywords** Parametric insurance · Basis risk · Open-source · Natural hazard · Tropical cyclone · European storm

## 1 Introduction

Insurance companies play a crucial role in financing rebuilding after devastating disasters caused by natural hazards. However, the difference between economic and insured damages, referred to as the insurance protection gap, has been growing over the past 40 years (Holzheu and Turner 2018). In light of this widening gap, parametric insurance provides an innovative solution with the potential to increase financial

security (Lin and Kwon 2020). This insurance scheme differs from the more common claim-based insurance, because it pays out when triggered by measured or modeled hydro-/meteorological parameters, instead of after a damage assessment (De Leeuw et al. 2014). Its advantages lie in low transaction costs, swift settlements (Barnett and Mahul 2007), and in its potential to make use of remote sensing data, which offers the opportunity to provide insurance coverage in inaccessible, isolated areas (De Leeuw et al. 2014). However, an important limitation to parametric insurance is the so-called basis risk, which describes the difference between the parameter-based payout and the actual damage. The payouts triggered by parametric insurance will always only be a proxy of the experienced damage. This stands in contrast to claim-based insurance, which bases payouts on incurred damages.<sup>1</sup> In the case of parametric insurance, the mismatch between proxy and damages can affect either the

✉ Carmen B. Steinmann  
carmen.steinmann@usys.ethz.ch

Benoît P. Guillod  
benoit.guillod@celsiuspro.com

Christopher Fairless  
chris.fairless@celsiuspro.com

David N. Bresch  
dbresch@ethz.ch

<sup>1</sup> Institute for Environmental Decisions, ETH Zurich, Universitätsstrasse 16, Zurich 8092, Zurich, Switzerland

<sup>2</sup> Federal Office of Meteorology and Climatology MeteoSwiss, Operation Center 1, Zurich-Airport 8058, Zurich, Switzerland

<sup>3</sup> CelsiusPro AG, Seebahnstrasse 85, Zurich 8003, Zurich, Switzerland

<sup>1</sup> Traditional claim-based insurances are often referred to as indemnity-based insurances. They make use of the observed damage as trigger for a payout (Jerry 2023). E.g. a flood height of 1 m might cause a damage of \$200'000 to a house with a total insured value of \$ 1 million. A claim-based insurance would first assess this damage and pay out the assessed amount of \$200'000. A parametric insurance on the other hand entails agreed flood heights at which a certain percentage of the total insured value is payout out. This could e.g. be 15% for a flood height of 1 m and therefore lead to an immediate payout of \$150'000.

policyholder who does not receive a payout despite experiencing damage or the insurance company if the policyholder receives a payout despite not having suffered any damage (Barnett and Mahul 2007). Therefore, a systematic approach to minimize basis risk is crucial to assess the viability of any parametric insurance product (Clement et al. 2018).

So far, parametric insurance and the related basis risk have mainly been studied in agriculture, as this is the sector for which this insurance scheme was first developed as an option to mitigate the risks of reduced yields due to natural hazards (Clement et al. 2018). In this field, scientists differentiate between three types of basis risk: Design basis risk arises from the inherent mismatch of the chosen parametric index being a proxy for the experienced damage. Temporal basis risk is related to the time period considered as one event leading to a payout. It is particularly relevant for seasonal parametric indices.<sup>2</sup> Lastly, spatial basis risk captures the distance between the measuring station and the farm location (Dalhaus and Finger 2016). In a review study, the authors find that most efforts to quantify basis risk in agriculture focus on analysing the correlation of the measured index at different weather stations (Clement et al. 2018), i.e. to quantify the spatial basis risk. These kind of systematic methodologies are not available across different natural hazards, affected exposures and basis risk types.

One important challenge in developing such systematic methodologies is the paucity in data availability and affordability, which also impedes the implementation potential of parametric insurance, particularly in the Global South. Insurance companies mostly operating in the Global North own claim data records and make use of vendor hazard models or perform risk assessments in-house. Low-income countries and stakeholders, however, are unable to afford setting up or purchasing this type of hazard model and do not have such detailed damage histories. In these cases open-source data can be crucial to design parametric insurance schemes. Figueiredo et al. (2018) set up a parametric insurance scheme using open-source data for both the natural hazard modeling and damage records and illustrate their approach with a case study in Jamaica. The authors use a logistic regression model to calibrate a parametric flood insurance model to damage data recorded by the International Disaster Database EM-DAT (Guha-Sapir et al. 2021). This approach provides a transparent framework to set up a parametric insurance scheme using only global open-source data, which renders it applicable beyond the illustrated case study. However, it still requires the user to build their own

hazard model, which constitutes an important barrier for its transfer to any different study region.

In this work we present a generalized framework for the design of parametric insurance schemes that is easily adaptable to different natural hazards and exposures. Moreover, we illustrate its implementation in the open-source risk assessment platform CLIMADA (Aznar-Siguan and Bresch 2019). Providing a globally consistent and spatially explicit approach enhances the ability to apply this methodology to a real world portfolio. We thereby improve the accessibility to, and the transparency of, such an innovative insurance scheme. Potential users from the public and private sector include the World Bank and the InsuResilience Solutions Fund, institutions which have already made use of CLIMADA in the past (Rana et al. 2022). Moreover, we illustrate the implementation in CLIMADA with two case studies: for tropical cyclones in Mozambique and for winter storms in France, both targeting hospitals. This study lays the foundations for further work and real-world applications and thereby contributes to closing the insurance protection gap.

## 2 Methods

We here propose a framework to globally consistently design parametric insurances (Sect. 2.1) and how this framework is implemented in the open-source risk assessment platform CLIMADA (Aznar-Siguan and Bresch 2019) (Sect. 2.2).<sup>3</sup> Finally, we introduce two case studies that are used to illustrate our approach in Sect. 2.3.

### 2.1 Framework

The Intergovernmental Panel on Climate Change (IPCC) defines the severity of an event as emerging from climate-related hazards; exposed human and ecological systems; and their vulnerability to the respective hazard (IPCC 2012):

$$\text{Damage} = F(\text{hazard, exposure, vulnerability}) \quad (1)$$

This concept has widely been taken up to study the damages caused by multiple hazards on different exposed entities (Ward et al. 2020). We here propose to transfer this damage assessment logic to the computation of payouts triggered by a parametric insurance scheme, given by

$$\text{Payout} = F(\text{parametric index, maximum payout, payout function}) \quad (2)$$

<sup>2</sup> A seasonal parametric index can e.g. be the cumulative amount of precipitation over the growing season. Temporal basis risk arises from the definition of the time period considered as the growing season.

<sup>3</sup> The code to set up and calibrate the parametric product options is freely and readily available at [https://github.com/CLIMADA-project/climada\\_papers/tree/main/202303\\_parametric\\_insurance\\_framework](https://github.com/CLIMADA-project/climada_papers/tree/main/202303_parametric_insurance_framework)

where the parametric index constitutes the analogy to the hazard; the maximum payout the analogy to the exposure and the payout function the analogy to the vulnerability.

The difference between damage and payout is used to quantify the basis risk as follows:

$$\text{Basis risk} = \text{Damage} - \text{Payout} \quad (3)$$

We discuss below the analogy of the components of Eqs. 1 and 2 (Sect. 2.1.1, 2.1.2 and 2.1.3). Section 2.1.4 describes in depth the following steps to design parametric insurance products and proposes how to overcome data scarcity.

- I. Choosing an adequate parametric index
- II. Acquiring historical time series and/or generating probabilistic time series of the parametric index suitable for a comprehensive risk assessment
- III. Acquiring historic damage records or estimates
- IV. Defining parametric product options (consisting of the combination of a parametric index and payout function)
- V. Choosing an optimization criterion and determining the best-fitting parametric product which minimizes the basis risk described in Eq. 3
- VI. Testing the resulting parametric product with historic events
- VII. (optional) Testing whether the chosen parametric product is also viable under climate change projections

### 2.1.1 Hazard — parametric index

Natural hazards are described by an intensity parameter which is best representative of potentially incurred damages on exposed entities. Examples of common intensities used for risk estimates are the maximum wind speed for storms (Eberenz et al. 2021; Welker et al. 2021) and the thermal anomaly of fires (Lüthi et al. 2021).

The parametric index represents the analogy to the hazard intensity. It is derived from a measured or modeled hydro-/meteorological parameter. Commonly it is either defined as event-based index for single events exceeding defined intensity thresholds (e.g. maximum precipitation) or as seasonal index (e.g. accumulated precipitation over a certain time period). Moreover, the index (catastrophe, short cat) is measured in a fixed geographical extent (commonly a box or circle). This results in insurance products known as cat-in-a-box or cat-in-a-circle. Within this spatial extent different statistical metrics can be chosen as representative index. Commonly used metrics include the average or maximum value of the hydro-/meteorological variable.

### 2.1.2 Exposure — maximum payout

The exposure represents all entities potentially exposed to hazards. It can be of monetary value, but can also represent e.g. the population exposed to a natural hazard (Aznar-Siguan and Bresch 2019).

Analogously to the exposure value being the maximum potential damage at every location, the maximum payout is the value at stake in the parametric insurance equivalent (commonly referred to as policy limit). The maximum payout represents the maximum value which a policyholder can expect to be covered by the parametric insurance within the agreed time frame. It can be used to transfer the risk of physical assets, but also of secondary losses such as business interruptions. The latter can be extended beyond direct physical damages to the insured property, although this is not yet part of standard business interruption insurances (Lin and Kwon 2020). A parametric insurance might for instance cover only part of the exposure value, especially if it serves as a complement to traditional (indemnity-based) insurance; hence the maximum payout can be set according to the taste of the insured. Note that generally local-level risk aggregates are a more appropriate target market for parametric insurance than individual households, as the basis risk can even out between the single entities of the risk pool (Barnett and Mahul 2007).

### 2.1.3 Vulnerability — payout function

The vulnerability of a given type of exposure (e.g. a building) represents its susceptibility to the hazard intensity. It is described by an impact function<sup>4</sup> which relates the intensity of the hazard with the percentage of the exposed value being damaged (mean damage degree (MDD)<sup>5</sup>) (Aznar-Siguan and Bresch 2019). Note that, depending on the type of hazard and exposure, the range of the MDD differs and might never reach 100% (total damage). For example, the maximum expected damage to physical assets (averaged over a risk portfolio) caused by winter storms in the Canton of Zurich, Switzerland, amounts to 5% of their total value (Welker et al. 2021). Ideally, impact functions are calibrated using historic hazard measurements and reported damage data.

In analogy to the impact function relating hazard intensity to the damage fraction of the exposed value, a payout function represents the relationship between the parametric index and the fraction of the maximum payout. This function is commonly described by a step or linear function (see

<sup>4</sup> We do not refer to this functional relationship as a 'damage function' in order to avoid confusion with the term being used in integrated assessment models (Stanton et al. 2009).

<sup>5</sup> The MDD is also referred to as expected damage ratio (EDR).

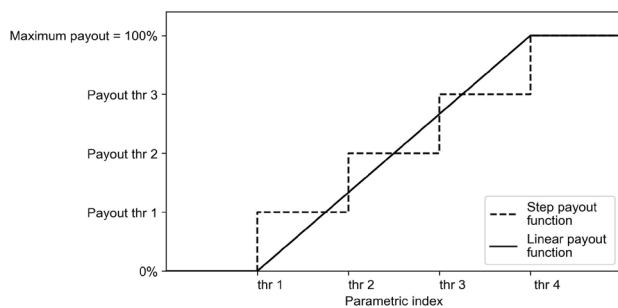


**Fig. 1** Schematic illustration of a step and linear payout function. Payout functions represent the relationship between a parametric index and a payout. A step payout function defines different parametric index thresholds (thrs) which trigger payout thrs. Linear payout functions assume a linear increase in payout between two index thr. The minimum payout amounts to 0% and the maximum to 100% of the maximum payout

Fig. 1), which is defined by one or several parametric index thresholds (thr) triggering a respective payout thr. In the case of a linear payout function, the increase in between two defined thresholds is linear. The minimum payout amounts to 0% and the maximum to 100% of the maximum payout.

#### 2.1.4 Designing parametric insurance products

There are a few points to consider when choosing a parametric index. The parametric index needs to be measurable in an objective manner, with an independent third party assessing payouts (Franco 2010). Common providers of such data are local weather services, space agencies (e.g. NASA) for satellite products, and agencies providing reanalysis data. Besides being a good damage proxy, the index also has to be available in near real-time (Figueiredo et al. 2018) to allow for a swift settlement of the payout. Moreover, insurance pricing is based on a comprehensive risk assessment, which requires to accurately model the distribution of the chosen index and its extreme values (Clement et al. 2018). One common limitation to accurately estimate this distribution statistically is the relatively short duration of historical hazard time series. This is particularly critical for the insurance sector as it focuses on extreme events, which are rare by nature. One robust way to overcome this limitation is to rely on probabilistic hazard models that adequately represent the tail risk and thereby allow to assess risk and determine pricing (Mitchell-Wallace et al. 2017). Lastly, a simple and transparent procedure is essential in the implementation of a parametric product (Franco 2010).

Once different parametric product options have been determined, systematic decision criteria are needed to assess the best suited product. To do so, we compute probabilistic payouts following Eq. 2 for different parametric product options and compare them to find the one best approximating

historic damages. For this reason, damage records are crucial to correctly estimate the relationship between parametric index and damages (Clement et al. 2018). Whenever available, damage records of the considered risk pool should be used for this analysis. In order to choose between different parametric products, different optimization criteria can be applied. They range from a binary hit-or-miss criterion (Figueiredo et al. 2018) to such that include the peak-over-threshold like the root mean squared error (RMSE). In contrast to the RMSE which weights events according to their impact, the root mean squared fraction (RMSF) (Eberenz et al. 2021) is an option that does not differentiate between events and weights them equally. Parametric insurance schemes are crucial to ensure liquidity (Van Nostrand and Nevius 2011), in particular after big events. This focus on events causing large impacts favours the use of the RMSE for optimization. Lastly, cost functions can be applied to optimize parametric insurance schemes (Brown and Carriquiry 2007), also.

#### 2.1.5 Testing climate resilience

Systematic methods to assess the resilience of parametric insurance products to climate change are important to evaluate their potential in risk transfer also in a changing climate (Clement et al. 2018). Already today human activities are responsible for a global warming of about 1.1 °C since pre-industrial levels. Moreover, the likelihood of reaching 1.5 °C in the near-term (2021–2040) exceeds a likelihood of 50% across climate change scenarios (IPCC 2021). This renders climate change driven projections relevant to the insurance sector to estimate today's risk accounting for past trends. For this reason, once the parametric product has been set up, it is worthwhile to make use of available future projections of hazard intensity and frequency, to test whether the chosen product still performs to a satisfactory degree under different degrees of global warming.

### 2.2 Implementation in CLIMADA

In this section we describe how functions and data sets available in CLIMADA can be used to design parametric products in a step-by-step process. We also provide a detailed tutorial for users to reproduce our methods and adapt them to their use cases.<sup>6</sup> We make use of probabilistic hazard sets which are readily available for tropical cyclones (TCs) (Eberenz et al. 2021) and European winter storms (Welker et al. 2021) via the CLIMADA data API.<sup>7</sup> Moreover, the

<sup>6</sup> [https://github.com/CLIMADA-project/climada\\_papers/tree/main/202303\\_parametric\\_insurance\\_framework](https://github.com/CLIMADA-project/climada_papers/tree/main/202303_parametric_insurance_framework)

<sup>7</sup> <https://climada.ethz.ch/data-types/>



CLIMADA data API provides two exposure layers used in this study. The first is the asset exposure data set LitPop, which globally consistently disaggregates asset value data proportional to a combination of nightlight intensity and geographical population data (Eberenz et al. 2020). The second exposure data set provides an interface to access OpenStreetMap (OSM) data (OpenStreetMap contributors 2017) in CLIMADA (Mühlhofer et al. 2023b). It contains different infrastructure components such as educational and healthcare facilities; roads and railways; and power lines. An additional module in CLIMADA maps these interdependent infrastructure networks and allows to compute cascading failures (Mühlhofer et al. 2023a). This module can be used to not only access direct physical damages to infrastructure, but also business interruptions due to propagating failures, such as power outages affecting hospitals (Mühlhofer et al. 2023c).

Exposure-specific damage records are often not available and incomplete, in particular in the Global South. Therefore, we here propose an approach to approximate these damage data. A global source of damage records is provided by EM-DAT (Guha-Sapir et al. 2021). EM-DAT reports the damages caused by major natural hazard events around the world. These records in combination with the LitPop exposure were used to calibrate impact functions for different natural hazards in CLIMADA (Eberenz et al. 2021; Lüthi et al. 2021). We use the resulting impact functions to compute *modeled damages*. We here assume that these *modeled damages* approximate the real damage caused to physical asset risk pools even when designing a parametric product for a sub sample of the total asset value contained in LitPop (whose vulnerability might deviate from the average impact function calibrated with LitPop).

We obtain different parametric product options by combining variations of parametric indices (differing in the covered spatial extent and the statistical metric) with a family of payout functions. For the spatial extent variations we provide the shapes of a box or circle; common dimensions are multiples of 10 km. For the family of payout functions we make use of existing categorization scales (SIMPSON and SAF-FIR 1974) for TC and multiples of 10 m/s for winter storms as index thresholds; and multiples of 10 or 25% for payout thresholds. The hazard set is divided into two subsets containing the historic and probabilistic events. The probabilistic sub set is used to compute *modeled damages* and *calculated payout* by combining hazard intensity/parametric index with the exposure/maximum payout and the impact function/payout functions respectively. The difference between the *modeled damages* and *calculated payouts* for each parametric product option across all probabilistic events results in the *modeled basis risk*. We here define the fittest parametric product (consisting of the combination of a chosen index and payout function) as the product that minimizes

the RMSE of *modeled basis risk*. Lastly, we compute the historic *modeled damages* and *calculated payouts* by combining the historic hazard set with the impact function/fittest parametric product; and test the climate resilience of the fittest product by computing *modeled damages* and *calculated payouts* for future projections. CLIMADA provides methods to compute these projections for TC (described in more detail in section 2.3.1), which renders this analysis easily accessible. Future projections for European storms are in preparation (Severino et al. 2023). In the following, we showcase the discussed methods with two illustrative case studies. We choose to present them for hazard, exposure and vulnerability combinations that are globally available in CLIMADA and thereby easily transferable to study regions beyond the ones shown here.

### 2.3 Illustrative case studies — hospital storm insurance

We here apply the presented framework to investigate storms affecting hospitals in different parts of the world. As a showcase results are analyzed in detail for hospitals in Mozambique. In 2019 Mozambique was listed as the country most affected by natural hazard extremes by the organization Germanwatch e.V. (Eckstein et al. 2021). That year the TCs Idai and Kenneth led to devastating damages, also with severe consequences for the health sector (UNDP 2019).

Moreover, the presented framework is easily transferable to any natural hazard (including different data sets for the same hazard type, future projections and different hazard types (such as wildfires (Lüthi et al. 2021))) and exposures globally. Within CLIMADA, the hazard object can simply be replaced before it is passed to the subsequent methods. For example, Meiler et al. (2022) compute and compare risk estimates for different TC hazard sets in CLIMADA. If a different hazard type is chosen, the vulnerability (impact function) and parametric index need to be adapted. In order to showcase the flexibility of our methodology, we set-up and optimize parametric insurance product options for hospitals in France as risk transfer measure against European winter storms. The required data sets are readily available on the CLIMADA data API, which makes this additional analysis relatively straightforward. Moreover, the user could implement any further hazard on this platform in order to follow the methodology presented in this work.

The exposure points represent hospital locations provided by OSM (OpenStreetMap contributors 2017) (see Section A in the Appendix for more details). In this stylized study every hospital location is assigned a value of 1 (hospital unit). In a real world application the hospital values can not only represent the value of the physical asset, but can also be set to the patient capacity, expected revenue or secondary costs (as basis for a balance sheet protection). As TCs can

lead to the complete destruction of physical assets (Eberenz et al. 2021), we set the maximum payout to 1 (hospital unit) for each hospital. This normalized hospital unit offers the opportunity to exemplify different *modeled damages* and *calculated payouts* caused by TCs and the wide range of insurance set ups that can be covered by parametric insurance (see examples in Table 1 in the Appendix).

### 2.3.1 Case study 1 — tropical cyclones in Mozambique

We use historic TC tracks (1980–2022) from the International Best Track Archive for Climate Stewardship (IBTrACS) (Knapp et al. 2010) and 9 perturbed tracks per historic storm (IBTrACS\_p) which were obtained by a direct random-walk process (Kleppek et al. 2008). The method to generate the perturbed IBTrACS\_p can be found in the supplementary material of Gettelman et al. (2018). Moreover, we here use improved perturbed tracks<sup>8</sup> that reduce the low intensity bias highlighted by Meiler et al. (2022). The maximum 1-minute sustained wind speed is commonly used as damage proxy for TC (Eberenz et al. 2021). To obtain this metric we compute one hazard footprint per track with the parametric wind field model proposed by Holland (2008). The parametric index is chosen as the maximum 1-minute sustained wind speed per event within a circle around each exposure point. For each index product, all circles (i.e., hospital locations) are assigned the same radius, ranging from 10 to 50 km (in 10 km steps), resulting in 5 different radii. In the following we will refer to these indices as x-km-cat-in-a-circle. IBTrACS data are updated twice a week, which ensures a rapid access to hazard records and thereby enables a swift settlement.

The payout function is set to a step function, where the index thresholds follow the TC Category-equivalent (Cat.) 2–5 following the Saffir–Simpson Hurricane Wind Scale (SSHWS) (SIMPSON and SAFFIR 1974). Throughout this paper we will refer to TCs by their equivalent SSHWS Cat.. The payout thresholds are set to multiples of 25%. This results in a payout function family for which each of the TC Cat.2–5 can give a payout of 0%, 25%, 50%, 75% or 100% of the maximum payout, as long as it is equal to or higher than the category below. This results in 70 payout functions, ranging from the TC Cat.2–5 all triggering 0% payout to all of them leading to a 100% payout.

The Post Disaster Needs Assessment (PDNA) of TC Iдай and Kenneth (UNDP 2019) lists the number of hospitals (see Table 2 in the Appendix) as well as the most affected regions in Mozambique. This information is used for a first qualitative analysis of our results. However, as these records only cover two events and no quantitative metrics such as

the type, location or degree of affected health facilities, we additionally compute *modeled damages* for a quantitative analysis of the *calculated payouts* and *modeled basis risk*. To compute the *modeled damages* we make use of a TC impact function calibrated on a basin level (Eberenz et al. 2021). The basin covering Mozambique is the 'South Indian Ocean'. We compute the *modeled damages* both for the historic and perturbed IBTrACS. This historic *modeled damages* can then be compared to aforementioned recorded impacts (in this case in form of affected regions listed in the PDNA).

For the quantitative analysis we additionally derive the *calculated payouts* for all parametric product options. These are obtained by combining the 5 parametric indices (radii) described in section 2.3.1 with the 70 members of the payout function family discussed in section 2.3.1, leading to 350 parametric product options. The *modeled basis risk* per perturbed track is calculated following Eq. 3 and summing over all affected hospitals. Subsequently, we compute the RMSE over all events for each parametric product and determine the best suited product as the one minimizing this value. In a second step the *modeled damages* and *calculated payouts* for the best fitting parametric product (the combination of a radius and member of the payout function family) are calculated for all historic events.

The IPCC<sup>9</sup> concludes that the spatial patterns of many variables depend mostly on the level of global warming, independent of the timing it is reached (IPCC 2021). For this reason, we choose to test the climate resilience of our approach by analyzing the two warming levels 1.5 °C and 2.5 °C.

The TC intensity and frequency are projected to change under climate scenarios. Knutson et al. (2015) propose correction factors for different basins that reflect these changes under RCP 4.5 at the end of the century. These correction factors as well as an interpolation for RCP 2.6 are implemented and easily applicable in CLIMADA. The correction factors for RCPs 2.6 and 4.5 at the end of the century correspond to the two chosen warming levels 1.5 °C and 2.5 °C. We here apply them to the perturbed IBTrACS\_p and determine the fittest parametric product option for future scenarios.

### 2.3.2 Case study 2 — winter storms in France

Moreover, we illustrate the flexibility of our methodology with a second case study using a different natural hazard

<sup>8</sup> [https://github.com/CLIMADA-project/climada\\_python/pull/688](https://github.com/CLIMADA-project/climada_python/pull/688)

<sup>9</sup> The IPCC assesses literature on climate risks. Beyond possible future climate change this includes societal development and responses. Climate model simulations are driven by different scenarios, covering both emission/concentration scenarios referred to as Representative Concentration Pathway (RCPs) and Shared Socioeconomic Pathways (SSPs) (IPCC 2021).

type. In this case we demonstrate the design of a parametric product for winter storms affecting hospital locations in France. Winter storms lead to significant impacts in Europe and are projected to increase in the future (Leckebusch et al. 2007). We here use historic wind gust footprints provided by the Windstorm Information Service (Copernicus WISC) and perturbed storms WISC\_p described in more detail in Schwierz et al. (2010). These hazard footprints have been used for risk analysis and are readily available on the CLIMADA data API (Welker et al. 2021). The WISC winter storm data set contains 142 historic storms for the time period 1940–2011 in France. Each historic storm is perturbed 29 times, resulting in 4118 synthetic storms WISC\_p. Moreover, there are 50 hospitals in the OSM data set (OpenStreetMap contributors 2017) in France, which are assigned a value of 1 hospital unit (HU) each. We make use of the impact function calibrated on insurance claims using LitPop (Eberenz et al. 2020) in the Canton of Zurich, Switzerland, by Welker et al. (2021). This function has a maximum MDD of 5%, which constitutes an important difference between the two presented case studies: While TCs can cause the total destruction of a physical asset, winter storms are assumed to lead to a maximum damage to physical assets of 5%. This results in a choice of maximum payout that does not correspond to the 100% of the physical asset value as was the case for the parametric product targeting TCs. Instead, in this case we set the maximum payout to 5% of the unit value, i.e. a maximum payout of 0.05 HU per location, resulting in a total maximum payout of 2.5 HU for the whole risk pool (containing all hospital locations in France). The parametric index is chosen as the maximum wind speed per event in a circle around each exposure point. Five different radii are chosen: 10–50 km. For the payout function we here choose 10 m/s steps as parametric index thresholds for maximum wind speeds between 40–60 m/s and 10% steps for the payout thresholds. This results in 286 payout functions and in combination with the radii in 1430 parametric product options. In Europe, different national weather agencies provide near-real-time data, which can be used for settlement. For example, the French national weather agency uses output from the AROME weather model (Seity et al. 2011).

### 3 Results

We here first show hazard maps for the most destructive event TC Idai overlaying the spatially distributed exposure to illustrate our approach in a spatially explicit manner. From there we present our quantitative analysis resulting in a parametric product for hospitals in Mozambique which reduces the RMSE for the *modeled basis risk*. Lastly, we showcase

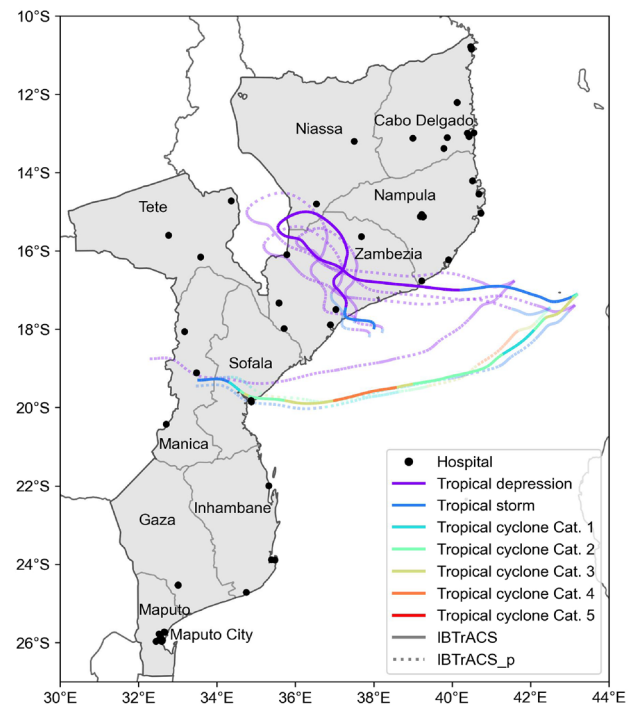


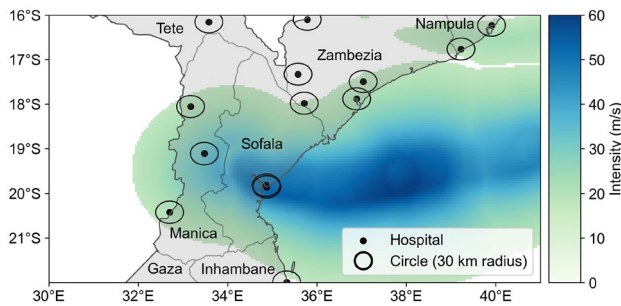
**Fig. 2** Tropical cyclone (TC) tracks over Mozambique and hospital locations. Historic IBTrACS (Knapp et al. 2010) track of TC Idai and for illustration 3 out of the 9 perturbations of the original track. Colors represent TC categories (Cat.) following the Saffir–Simpson Hurricane Wind Scale (SIMPSON and SAFFIR 1974); the solid line illustrates the historic track and dashed lines the perturbed ones. Black points depict hospital locations (OpenStreetMap contributors 2017)

how our approach can be transferred to hospitals affected by winter storms in France.

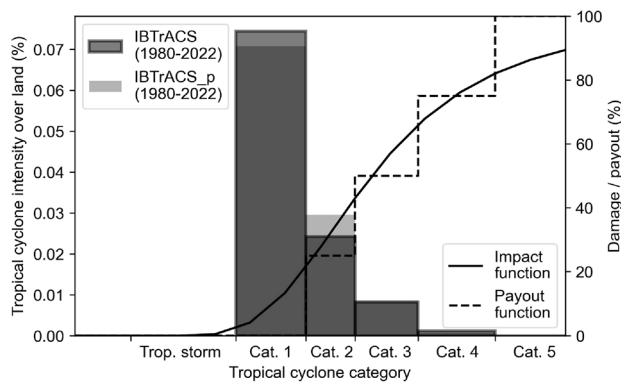
#### 3.1 Case study 1 — tropical cyclones in Mozambique

Figure 2 shows the historic and for illustration 3 out of the 9 perturbed tracks of TC Idai as well as the spatial distribution of hospitals across Mozambique. Idai formed in front of the coast of the region of Zambezia as a tropical depression, made landfall, then traversed towards the sea, subsequently re-emerged, and ultimately struck the regions of Sofala and Manica with much higher intensities (up to TC Cat.3).

The historic track of Idai is the base to compute the TC wind field shown in Fig. 3. We here illustrate the maximum 1-minute sustained wind speed ( $\geq 17.5$  m/s) over the most affected regions of Central Mozambique. Moreover, we show OSM hospital locations (OpenStreetMap contributors 2017); and circles around them representing one of the spatial extents chosen to assess the parametric index (radius 30 km). Hospitals exposed to the highest TC wind speeds (60 m/s) are located in the region Sofala. Other hospital



**Fig. 3** The hazard footprint of the maximum 1-minute sustained wind speed (m/s) of tropical cyclone Idai over the Central regions of Mozambique (for wind speeds  $\geq 17.5$  m/s). The track is extracted from IBTrACS (Knapp et al. 2010) and the wind field computed using the Holland (2008) wind field model. Black points represent hospital locations (OpenStreetMap contributors 2017) and the circles represent the considered spatial extent of a cat-in-a-circle parametric product with a radius of 30 km



**Fig. 4** Histograms of on-land tropical cyclone (TC) wind speeds in Mozambique; impact and payout function. The left y-axis displays the percentage of two histograms of wind speeds. They contain the percentage of land centroids affected by wind speeds belonging to bins per TC category (Cat.) following the Saffir–Simpson Hurricane Wind Scale (SIMPSON and SAFFIR 1974): the dark grey histogram represents historic IBTrACS (Knapp et al. 2010) and the light grey one perturbed IBTrACS\_p, both for the time period 1980–2022. The right y-axis contains the percentage of modeled damages or calculated payouts as a function of the TC Cat. The solid line represents the regional impact function of the basin 'South Indian Ocean' (Eberenz et al. 2021) and the dashed line depicts one of the two best fitting payout functions (which minimizes modeled basis risk for RMSE) and utilizes a cat-in-a-circle with a radius of 10 km. The impact and payout function were both applied to the same exposure/maximum payout, which constitutes a special case described in more depth in section 2.3.1

locations that overlay with the TC footprint stand in the regions Manica, Zambezia and Nampula. One hospital in the region of Inhambane does not coincide with the hazard footprint, however, the circle around it does. This is an example for the parametric index having a value greater than zero although no wind speed is assigned to the exposure point.

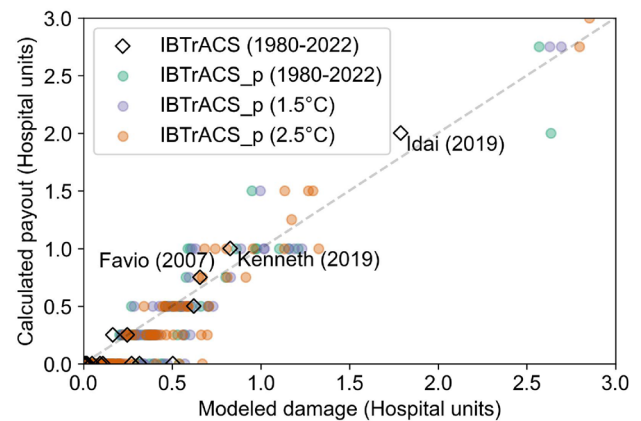


**Fig. 5** Tropical cyclones modeled damages vs. calculated payouts in hospital units in Mozambique. Results are shown for historic IBTrACS (1980–2022) (Knapp et al. 2010), and perturbations of the historic tracks IBTrACS\_p under different climatic conditions (historic (1980–2022), 1.5 °C, 2.5 °C). We highlight the three largest historic events Idai (2019), Kenneth (2019) and Favio (2007). The dashed diagonal represents a perfect agreement between the modeled damages and calculated payouts and thereby a modeled basis risk of zero

The wind field computation is conducted for 70 historic IBTrACS (1980–2022) as well as for 615 perturbed tracks IBTrACS\_p over Mozambique. In Fig. 4 we present the distribution of TC intensity over land per TC Cat. (Cat.1–5) for both of those hazard sets. Figure 4 illustrates that land grid cells are subjected to TCs of Cat.1–4 to a decreasing degree. The IBTrACS\_p hazard set contains less cells affected by Cat.1 and more impacted by Cat.2 than the historic set. Both hazard sets do not entail any TCs of Cat.5 on land in Mozambique. Additionally, Fig. 4 illustrates the regionally calibrated TC impact function for the basin 'South Indian Ocean' (Eberenz et al. 2021); and a member of the payout function family. This payout function is part of one of the two fittest parametric product options, which have the lowest modeled basis risk. The modeled basis risk is defined as minimizing the RMSE between calculated payouts and modeled damages. Both of those parametric products were computed using a 10-km-cat-in-a-circle. Their payout function family members only differ in the payout triggered by a TC of Cat.5. While one remains at a payout of 75% of the maximum payout, the other (shown here) increases to 100% for TC Cat.5. Both products resulting in the same RMSE can be explained by no events reaching Cat.5 on land in Mozambique.

In the following, we apply the impact function/payout function shown in Fig. 4 to the hazard intensity/10-km-cat-in-a-circle to compute modeled damages/calculated payout. Figure 5 opposes these two. The results are displayed in hospital units (HU), which sum up the damages caused to different hospitals (that were all assigned a value of 1 HU). The dashed diagonal represents a perfect agreement between



*modeled damages* and *calculated payouts* and therefore a *modeled basis risk* of zero. Besides the perturbed tracks IBTrACS\_p (1980–2022) used for calibration, we here highlight historic events and in particular the three largest historic TCs Idai (2019), Kenneth (2019) and Favio (2007). In the case of Idai our computation lead to *modeled damages* in the regions Sofala (accounting for 1.73 HU) and Manica (0.05 HU). For TC Kenneth all damages are modeled in Cabo Delgado (0.83 HU). The normalized unit of HU can be used to compute *modeled damages* and *calculated payouts* in different units. Moreover, the exposure and maximum payout do not have to be set to the same value, but can be defined independently from one another. For demonstration we here present two examples based on damage records from the PDNA (UNDP 2019) (see Table 1 in the Appendix). The first example assumes that the asset value of each hospital amounts to \$45 million and is protected by a maximum payout of \$20 million per HU. This leads to *modeled damages* of \$80.6 million and *calculated payouts* of \$40 million for the historic event Idai. The second example assumes disaster response efforts as a function of population loosing access to a hospital. In this simple example we assume the total population of Mozambique to be equally distributed between hospital units. Moreover, we assume a parametric coverage of \$50 per person loosing access to a hospital. This example results in 832'642 people loosing access to a hospital and a *calculated payout* of \$46.5 million.

Additionally, Fig 5 includes the results for modified tracks representing warming levels of 1.5 °C and 2.5 °C. For both projections the same parametric product option remains the fittest. Across scenarios we observe that whereas *modeled damages* vary smoothly (scatter distribution in x-direction), they show jumps in *calculated payout* in multiples of 0.25 HU (y-direction), which reflect the definition of the payout function family as increasing in multiples of 25%. Moreover, the greatest mismatch between *modeled damages* and *calculated payouts* prevails for small *modeled damages* (0–0.5 HU), which often do not receive any payout. We investigate the distribution of cases experiencing certain damages and receiving certain amounts of payout in more detail for the perturbed track set. Figure 6 illustrates the distribution of *calculated payout* received by cases experiencing a certain amount of *modeled damages*. Cases in which an event leads to *modeled damages* at a hospital location are divided in bins with a step width of 10%. Most cases lead to *modeled damages* and *calculated payouts* between 0 and 10% (324 cases). In 44 cases hospitals experience *modeled damages* of 10–20% during an event. Out of these units 65% receive no (0%) *calculated payout* and the remaining 35% of units obtain 25% of *calculated payout*. This results in a mean *calculated payout* of 8% across all cases. The mean *modeled damages* in this bin amounts to 13%. The number of cases decreases for bins containing larger *modeled damages*. For

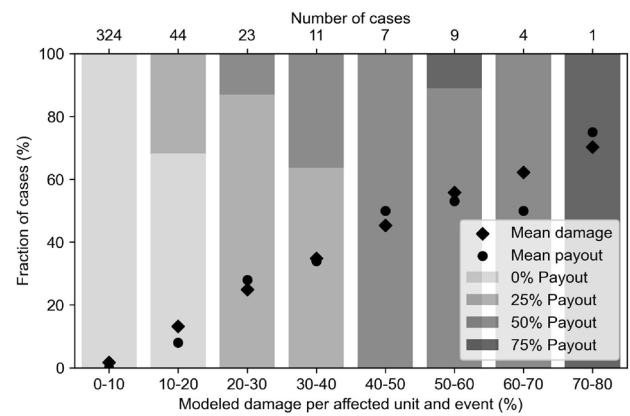


**Fig. 6** Fraction of *modeled damage* cases receiving a certain *calculated payout*. The *modeled damages* are split in bins (lower x-axis, 10% steps) and the y-axis shows the fraction of cases receiving a certain amount of *calculated payout* (in bins of 25% step width) for historic perturbed IBTrACS\_p (1980–2022) in Mozambique. The upper x-axis displays the number of cases belonging to each *modeled damage* bin. The mean *modeled damages* and *calculated payout* are displayed per *modeled damage* bin (scatter points)

most bins the mean *modeled damage* and mean *calculated payout* amount to a similar value, except for the bin containing 4 cases leading to *modeled damages* between 60 and 70%. In this case the mean *modeled damage* amounts to 62% and the mean *calculated payout* to 50%.

To summarize, the here presented framework is capable to support the selection of the best-fitting parametric product option in terms of minimizing *modeled basis risk* and allows for testing the climate sensitivity of the structure, too.

### 3.2 Case study 2 — winter storms in France

Here, we showcase how our approach can be transferred to design parametric insurance products for a different hazard type. We determine the fittest parametric product option to cover hospitals in France against damages from winter storms. Figure 7 shows the distribution of winter storm intensity ( $\geq 40$  m/s) over land in France for 142 historic WISC storms (1940–2011) and 4118 perturbed storms WISC\_p. It illustrates that land grid cells are subjected to winter storms reaching wind gusts up to 55 m/s. The distribution of winter storm intensity is nearly identical between the historic and perturbed storms with slightly more cells affected by wind speed between 40–45 m/s in the historic set and slightly more cells subjected to wind speeds between 45–50 m/s in the perturbed set. Moreover, Fig. 7 depicts the impact function calibrated by Welker et al. (2021) and a member of the payout functions family. This payout function is one of the ten fittest parametric product options which minimize the *modeled basis risk* (here the RMSE between *modeled damages* and *calculated payouts*). All of those

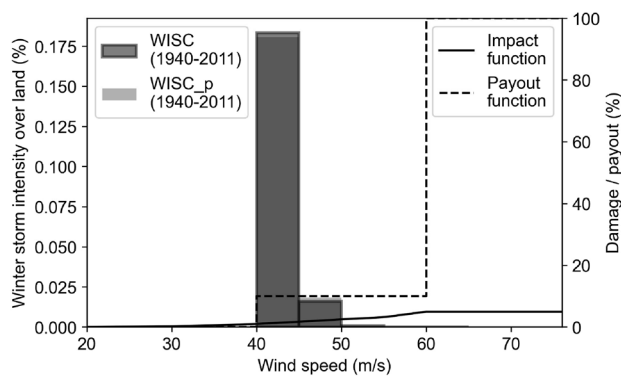


**Fig. 7** Histograms of on land winter storm intensity ( $\geq 40$  m/s) in France; impact and payout function. The left y-axis displays the percentage of two histograms of wind speeds. They contain the percentage of land grid cells affected by wind speeds belonging to 5m/s bins: the dark grey histogram represents historic WISC storms and the light grey one perturbed WISC\_p, both for the time period 1941–2011 (Schwierz et al. 2010). The right y-axis contains the percentage of modeled damages or calculated payouts as a function of the wind speed. The solid line represents the impact function (Welker et al. 2021) and the dashed line depicts one of the ten fittest payout functions (which minimize modeled basis risk for RMSE) and utilizes a cat-in-a-circle with a radius of 10 km. The impact function and payout function were applied to different exposure/maximum payout values, which constitutes a special case described in more depth in section 2.3.2

parametric products are computed using a 10-km-cat-in-a-circle. They result in a payout of 10% for the index thresholds 40 and 50 m/s and differ only for the payout triggered by gusts of 60 m/s paying out 10–100% of the maximum payout. Here, we show the payout function increasing to 100% for wind gusts of 60 m/s. The maximum payout in this example amounts to 5% of the exposure value, which means that although impact and payout function are displayed on the same scale (0–100%), these fractions imply different absolute values.

## 4 Discussion

In this work we illustrate how parametric insurance products can be designed using the same model framework as for damage estimates and by reducing (modeled) basis risk. We provide a systematic approach that can be applied globally across hazards and exposures. The dissemination of this innovative insurance scheme also to the Global South is eased by providing open-source global probabilistic hazard sets and an open-access code base.

With respect to the case study in Mozambique Fig. 4 illustrates that the distribution in TC intensity over land in Mozambique is similar for the historic and perturbed IBTrACS. The perturbed tracks show slightly less TC Cat.1 and more Cat.2, which suggests an improvement to the

previously reported low-intensity bias (Meiler et al. 2022). The PDNA on TC Idai and Kenneth in Mozambique (UNDP 2019) constitutes a point of reference to qualitatively ground the chosen exposure data set and modeled damages. The total number and type of hospitals in the OSM data set (OpenStreetMap contributors 2017) are well in accordance with the records in the PDNA (see Table 2 in the Appendix). The damages of TC Idai and Kenneth are only reported for the number of health facilities affected and not specified for hospitals in the PDNA. In a real world application e.g. in collaboration with governmental institutions, quantitative damage records on regional level would likely be available. As a first approximation we here compare affected regions in our model and the PDNA. In the case of TC Idai we compute modeled damages in 2 (Sofala, Manica) out of the 5 (Sofala, Manica, Zambezia, Tete, Inhambane) regions listed in the PDNA. The regions Tete and Inhambane are not even exposed to wind speeds  $\geq 17.5$  m/s in our model. This suggests that damages might have been caused by TC flood sub-hazards (storm surge and torrential rainfall) and highlights the limitation of using wind as sole proxy for all damages (Bloemendaal et al. 2021). This is particularly important because the effects of climate change on TC sub-hazards may vary (Emanuel 2017; Knutson et al. 2020). Another possible explanation are damages resulting from cascading failures of interconnected infrastructures (Mühlhofer et al. 2023c). In the case of TC Kenneth both our model and the PDNA reflect Cabo Delgado as the most affected region.

Our quantitative analysis shows how the presented framework supports the selection of the fittest parametric product option in terms of minimizing modeled basis risk across future projections and natural hazards. Figure 5 reflects a low modeled basis risk (distance to dashed line) obtained for the fittest parametric product option, both for the perturbed tracks used in determining this product and the historic IBTrACS. Although tracks under climate change scenarios lead to higher modeled damages, the respective calculated payouts increase as well, resulting in similar estimates of modeled basis risk and suggesting some climate resilience of the chosen parametric product. Small modeled damages not receiving any calculated payouts can be explained by the impact function computing damages for TC Cat.1 and the payout functions family being restrained to only starting to pay out for TC  $\geq$  Cat.2 (see Fig. 4). This is in accordance with assuring liquidity (Van Nostrand and Nevius 2011) across the risk pool after events impacting single entities to a significant degree, which is a primary goal of parametric insurance. Figure 6 illustrates that risk aggregates are a more appropriate target market for parametric insurance than individual exposure points (Barnett and Mahul 2007). Even though in individual cases the calculated payout might not correspond to the modeled damages, their means across the risk pool result in a similar amount. However, local risk

pools can still be vulnerable to correlated weather extremes affecting the whole pool (Barnett and Mahul 2007). Therefore, future studies should investigate the potential of diversifying parametric insurance across regions, a concept that has shown to benefit risk pools (Ciullo et al. 2023). As parametric insurance is particularly susceptible to locally correlated extremes, it could not only benefit from but also facilitate the adoption of such diversified risk pools. Lastly, we show how our approach can be transferred to other natural hazards by applying it to winter storms in France. Fig 7 illustrates how choosing a maximum payout not amounting to the same value as the exposure (but to 5% of the exposure value) leads to a clear difference between impact and payout function. This stands in contrast to the impact and payout function for TC (Fig. 4), which cover similar damage/payout fractions in function of the their index, as they are defined on the same exposure/maximum payout value. The second case study on winter storms illustrates the flexibility of our approach, which can be tailored to suit different hazards and exposures/maximum payouts. In the future, this methodology could be further developed to provide coverage for multi-hazard risks (Stalhandske et al. 2023).

Damage reports such as the PDNA give an indication on historic damages, however, more detailed damage records are sparse, especially in the Global South. The paucity of appropriate damage data leads to the main limitation of the presented case studies, which is to model both the damages and payouts. This results in computing the *modeled basis risk* (with *modeled damages*) instead of an actual representation of basis risk with real damage data. For example, the best fitting index resulting in the maximum wind speed in a circle with the smallest tested radius (10 km) is most likely inherent to the approach, as the *modeled damages* use the maximum wind speed at the closest grid cell, and the parametric index uses the maximum wind speed of the cells within the radius. The smaller the radius, the closer the wind speed values are to the one at the exposed location. This is also reflected in the payout function approximating a discretization of the impact function (Fig. 4), which is additionally linked to the exposure and maximum payout amounting to the same value in the TC case study. (This constitutes a special case described in more detail in the previous section.) The *modeled damages* are computed using impact functions, which were calibrated using the LitPop exposure (Eberenz et al. 2020) and either EM-DAT records (Guha-Sapir et al. 2021) (in the case of TCs) or insurance claims data (Welker et al. 2021) (in the case of European winter storms). This renders a coarse representation of vulnerability, which might deviate considerably from the vulnerability of hospitals to these hazards. Also in traditional risk estimates the vulnerability constitutes a major uncertainty (Kropf et al. 2022). Besides quantifying related uncertainties (Kropf et al. 2022), users might choose to apply conservative impact functions (e.g.

the upper quantile provided by Eberenz et al. (2021)) instead of the best fitting impact function. The used impact functions constitute an important source of uncertainty in the presented work. However, they simultaneously provide a starting point for studies in data scarce regions and were systematically derived in a globally consistent way using open-source data.

The quantification and management of different types of basis risk (spatial, temporal, design (Dalhaus and Finger 2016)) are important to ensure the viability of parametric products (Clement et al. 2018). Spatial basis risk can be reduced by making use of cat-in-a-box/cat-in-a-circle products, which even out spatial variability. Moreover, considering the parametric index in a wider extent around the exposure can help to provide coverage for cascading effects such as the inaccessibility to hospitals due to the destruction e.g. of roads (Mühlhofer et al. 2023c). Taking into account not only direct physical damages, but also secondary effects can result in innovative business interruption insurance schemes (Lin and Kwon 2020). In terms of the temporal basis risk, the event definition is an important factor. Temporal basis risk results e.g. from the measurement time window of seasonal parametric indices usually being kept constant between years which disregards inter-annual variability. This is of particular importance for seasonal indices, e.g. covering reduced yields due to droughts (Dalhaus and Finger 2016). In this work we assess single storm events independently. However, storms might form clusters (Priestley et al. 2017), which might be assessed as one event by insurance products. Ultimately, the decision on which time frame to consider is strongly linked to the recovery period of the affected system between consecutive events (de Ruiter et al. 2020). For reducing design basis risk it is important to represent the different processes driving damage, and to reduce biases and capture as much variance as possible. For example, variables approximating flood sub-hazards could be included in parametric TC insurance products. To do so, one could base the parametric index on a TC categorization that takes into account all TC sub-hazards such as the scale proposed by Bloemendaal et al. (2021). Besides basis risk also pricing negotiations and other financial considerations influence the design of parametric insurance and should be considered in further work. High-resolution data can, for example, be used to study the effectiveness of parametric index options in hedging damages, as illustrated by Cummins et al. (2004). In that study, the authors make use of a TC vendor model and high resolution residential housing insurance data with a coverage of 93% in Florida. This allows them to determine the most adequate parametric index for insurances of different size to minimize basis risk. Other possible extensions include utility maximum considerations (Figueiredo et al. 2018; Zhang et al. 2019), and the pricing of hazard bonds (Chang et al. 2022).

Parametric insurances have the potential to contribute to closing the insurance protection gap. However, we need

**Table 1** For demonstration purposes: The application of the normalized 'hospital unit' to real world applications, describing an exposure per HU such as the physical asset value or the patient capacity. This exposure is then covered by a monetary maximum payout, which does not need to amount to the full amount in case the exposure is given in monetary unit. We here assume that all hospitals have the same value and choose it so the resulting *modeled damages* equal

	Total values	
	Exposure (\$45 million/HU; 465'163P/HU)	Maximum payout (\$20 million/HU; \$50/person)
Hospital Units (HU)	60HU	60HU
Asset value	\$45 million/HU*60HU = \$2.7 billion	\$20 million/HU*60HU = \$1.2 billion
Population	465'163P/HU*60HU = 27'909'798P	\$50/P*465'163P/HU*60HU = \$1.4 billion
Idai (2019)		
	<i>Modeled damages</i>	<i>Calculated payout</i>
HU	1.79HU	2HU
Asset value	\$45 million/HU*1.79HU = \$80.6 million	\$20million/HU*2HU = \$40 million
Population	465'163P/HU*1.79HU = 832'642P 832'642P*\$60.5/P = \$50.4 million	465'163P/HU*2HU = 930'326P \$50/P*930'326P = \$46.5 million

**Table 2** Number of hospitals per type in Mozambique in OpenStreetMap (OpenStreetMap contributors 2017) and the Post Disaster Needs Assessment (PDNA) of the tropical cyclones Idai and Kenneth (UNDP 2019)

Type of hospital	OpenStreetMap	PDNA
Central	4	4
Provincial	4	8
Military	2	2
General	6	7
District	14	24
Rural	10	19
Other	20	—
Total number	60	64

systematic methods for their design and to quantify basis risk across natural hazards and exposures. Using open-source data in the design process renders this innovative insurance scheme accessible to many actors, in particular, those from the Global South. In this work, we create and implement a framework to depict the relevant relationships and design parametric products. The method follows the same model framework used for damage estimates and uses open-source data across hazard types and future scenarios. Moreover, we provide an open-source and open-access code base,<sup>10</sup> which is easily adaptable to other input data. The main barrier to the implementation of parametric insurance is the paucity of damage records and the resulting coarse calibration of impact functions in data scarce

the damage records in the PDNA (UNDP 2019). The PDNA reports total health care infrastructure damages of \$81.5 million, and \$109 million in disaster response efforts accommodating the needs of 1.8 million people affected by the TC Idai, leading to an average cost of \$60.5/affected person. Considering a total population of 27'909'798 (UNDP 2019) and an equal distribution among the 60 hospitals, 465'163 people are assigned to each hospital

areas. The functions used in this work constitute a starting point in these cases and can be improved further if users provide damage records. Our methodology, along with the openly provided code and data form the basis for real-world applications. By doing so, we aim to make a meaningful contribution towards enhancing the resilience of our societies.

## Appendix A: Hospitals in the PDNA

The OSM data base (OpenStreetMap contributors 2017) contains 60 locations, which can be identified as hospitals by filtering them for those with a recorded name containing the word 'hospital'. Table 2 shows the number of these hospitals belonging to different sub types contained by OSM and the PDNA (UNDP 2019). The latter amount to 64 in Mozambique. Most hospitals belonging to higher-level administrative levels (such as central, provincial, general and military hospitals) can be identified in the OSM data set. Compared to the hospital locations, the number of health care facilities in general are not comparable in the two sources (1,157 in OSM; 8,425 in the PDNA).

**Acknowledgements** We would like to express our sincere appreciation to Alessio Ciullo for his insightful contributions and participation in discussions during the development of this research.

**Author contributions** CBS, BPG and DNB designed the analysis and the methodology, CBS conducted the analysis, analysed the results and generated the figures, CBS wrote the manuscript. All authors (CBS, BPG, CF and DNB) reviewed and edited the manuscript.

**Funding** Open access funding provided by Swiss Federal Institute of Technology Zurich. The research leading to these results received

<sup>10</sup> [https://github.com/CLIMADA-project/climada\\_papers/tree/main/202303\\_parametric\\_insurance\\_framework](https://github.com/CLIMADA-project/climada_papers/tree/main/202303_parametric_insurance_framework)



funding from the Swiss Innovation Agency Innosuisse under Grant Agreement No 53733.1 IP-SBM.

**Data availability** Historic IBTrACs, WISC and perturbed WISC storms are available through the CLIMADA data API <https://climada.ethz.ch/data-types/>. Map data copyrighted OpenStreetMap contributors and available from <https://www.openstreetmap.org> (OpenStreetMap contributors 2017).

**Code availability** The analysis were conducted using the Python tool CLIMADA, available at [https://github.com/CLIMADA-project/climada\\_python/](https://github.com/CLIMADA-project/climada_python/) (a frozen version was made available at <https://doi.org/10.5281/zenodo.6807463>). The code to generate the perturbed TC tracks is available under [https://github.com/CLIMADA-project/climada\\_python/pull/688](https://github.com/CLIMADA-project/climada_python/pull/688). A tutorial on how to use OSM data in CLIMADA can be found under [https://github.com/CLIMADA-project/climada\\_petals/blob/main/doc/tutorial/climada\\_exposures\\_openstreetmap.ipynb](https://github.com/CLIMADA-project/climada_petals/blob/main/doc/tutorial/climada_exposures_openstreetmap.ipynb). In particular, the code to set up and calibrate the parametric product options is freely available at [https://github.com/CLIMADA-project/climada\\_papers/tree/main/202303\\_parametric\\_insurance\\_framework](https://github.com/CLIMADA-project/climada_papers/tree/main/202303_parametric_insurance_framework).

## Declarations

**Conflict of interest** The authors declare no financial or personal interests that could be perceived as competing.

**Ethical approval** Not applicable

**Consent to participate** Not applicable

**Consent for publication** Not applicable

**Open Access** This article is licensed under a Creative Commons Attribution 4.0 International License, which permits use, sharing, adaptation, distribution and reproduction in any medium or format, as long as you give appropriate credit to the original author(s) and the source, provide a link to the Creative Commons licence, and indicate if changes were made. The images or other third party material in this article are included in the article's Creative Commons licence, unless indicated otherwise in a credit line to the material. If material is not included in the article's Creative Commons licence and your intended use is not permitted by statutory regulation or exceeds the permitted use, you will need to obtain permission directly from the copyright holder. To view a copy of this licence, visit <http://creativecommons.org/licenses/by/4.0/>.

## References

- Aznar-Siguan G, Bresch DN (2019) CLIMADA v1: a global weather and climate risk assessment platform. *Geosci Model Dev* 12(7):3085–3097. <https://doi.org/10.5194/gmd-12-3085-2019>
- Barnett BJ, Mahul O (2007) Weather index insurance for agriculture and rural areas in lower-income countries. *Am J Agric Econ* 89(5):1241–1247
- Bloemendaal N, de Moel H, Mol JM et al (2021) Adequately reflecting the severity of tropical cyclones using the new tropical cyclone severity scale. *Environ Res Lett* 16(1):014048. <https://doi.org/10.1088/1748-9326/abd131>
- Brown C, Carriquiry M (2007) Managing hydroclimatological risk to water supply with option contracts and reservoir index insurance. *Water Resour Res*. <https://doi.org/10.1029/2007WR006093>
- Chang CW, Chang JSK, Yu MT (2022) Pricing Hurricane bonds using a physically based option pricing approach. *N Am Actuar J* 26(1):27–42. <https://doi.org/10.1080/10920277.2020.1824798>
- Ciullo A, Strobl E, Meiler S et al (2023) Increasing countries' financial resilience through global catastrophe risk pooling. *Nat Commun* 14(1):922. <https://doi.org/10.1038/s41467-023-36539-4>
- Clement KY, Wouter Botzen WJ, Brouwer R et al (2018) A global review of the impact of basis risk on the functioning of and demand for index insurance. *Int J Disaster Risk Reduct* 28:845–853. <https://doi.org/10.1016/j.ijdr.2018.01.001>
- Cummins J, Lalonde D, Phillips RD (2004) The basis risk of catastrophic-loss index securities. *J Financ Econ* 71(1):77–111. [https://doi.org/10.1016/S0304-405X\(03\)00172-7](https://doi.org/10.1016/S0304-405X(03)00172-7)
- Dalhaus T, Finger R (2016) Can gridded precipitation data and phenological observations reduce basis risk of weather index-based insurance? *Weather Climate Soc* 8(4):409–419. <https://doi.org/10.1175/WCAS-D-16-0020.1>
- De Leeuw J, Vrieling A, Shee A et al (2014) The potential and uptake of remote sensing in insurance: a review. *Remote Sens* 6(11):10888–10912. <https://doi.org/10.3390/rs61110888>
- de Ruiter MC, Couasnon A, van den Homberg MJC et al (2020) Why we can no longer ignore consecutive disasters. *Earth's Futur* 8(3):e2019EE001425. <https://doi.org/10.1029/2019EF001425>
- Eberenz S, Stocker D, Rösli T et al (2020) Asset exposure data for global physical risk assessment. *Earth Syst Sci Data* 12(2):817–833. <https://doi.org/10.5194/essd-12-817-2020>
- Eberenz S, Lüthi S, Bresch DN (2021) Regional tropical cyclone impact functions for globally consistent risk assessments. *Nat Hazards Earth Syst Sci* 21(1):393–415. <https://doi.org/10.5194/nhess-21-393-2021>
- Eckstein D, Künzel Vera, Schäfer Laura (2021) Global Climate Risk Index 2021. Who suffers Most from Extreme Weather Events? Weather-related Loss Events in 2019 and 2000 to 2019. Germanwatch eV <https://www.germanwatch.org/en/19777>
- Emanuel K (2017) Assessing the present and future probability of Hurricane Harvey's rainfall. *Proc Natl Acad Sci* 114(48):12681–12684. <https://doi.org/10.1073/pnas.1716222114>
- Figueiredo R, Martina MLV, Stephenson DB et al (2018) A probabilistic paradigm for the parametric insurance of natural hazards. *Risk Anal* 38(11):2400–2414. <https://doi.org/10.1111/risa.13122>
- Franco G (2010) Minimization of trigger error in cat-in-a-box parametric earthquake catastrophe bonds with an application to Costa Rica. *Earthq Spectra* 26(4):983–998. <https://doi.org/10.1193/1.3479932>
- Gottelman A, Bresch DN, Chen CC et al (2018) Projections of future tropical cyclone damage with a high-resolution global climate model. *Clim Change* 146(3):575–585. <https://doi.org/10.1007/s10584-017-1902-7>
- Guha-Sapir D, Below R, Hoyois P (2021) EM-DAT: The CRED/OFDA International Disaster Database - [www.emdat.be](http://www.emdat.be) - Université Catholique de Louvain - Brussels - Belgium
- Holland G (2008) A revised Hurricane pressure-wind model. *Mon Weather Rev* 136(9):3432–3445. <https://doi.org/10.1175/2008MWR2395.1>
- Holzheu T, Turner G (2018) The natural catastrophe protection gap: measurement, root causes and ways of addressing underinsurance for extreme Events†. *Geneva Papers Risk Insur Issues Prac* 43(1):37–71. <https://doi.org/10.1057/s41288-017-0075-y>
- IPCC (2012) Managing the risks of extreme events and disasters to advance climate change adaptation: special report of the intergovernmental panel on climate change. Cambridge University Press, Cambridge
- IPCC (2021) Climate Change 2021: the physical science basis. Contribution of working group I to the Sixth assessment report of the

- intergovernmental panel on climate change. Cambridge University Press, Cambridge. <https://doi.org/10.1017/9781009157896>
- Jerry RH (2023) Understanding parametric insurance: a potential tool to help manage pandemic risk. In: Muñoz Paredes ML, Tarasiuk A (eds) Covid-19 and insurance. Springer International Publishing, Cham, pp 17–62
- Kleppek S, Muccione V, Raible CC et al (2008) Tropical cyclones in ERA-40: a detection and tracking method. *Geophys Res Lett*. <https://doi.org/10.1029/2008GL033880>
- Knapp KR, Kruk MC, Levinson DH et al (2010) The international best track archive for climate stewardship (IBTrACS): unifying tropical cyclone data. *Bull Am Meteorol Soc* 91(3):363–376. <https://doi.org/10.1175/2009BAMS2755.1>
- Knutson TR, Sirutis JJ, Zhao M et al (2015) Global projections of intense tropical cyclone activity for the late twenty-first century from dynamical downscaling of CMIP5/RCP4.5 scenarios. *J Clim* 28(18):7203–7224. <https://doi.org/10.1175/JCLI-D-15-0129.1>
- Knutson T, Camargo SJ, Chan JCL et al (2020) Tropical cyclones and climate change assessment: part II: projected response to anthropogenic warming. *Bull Am Meteorol Soc* 101(3):E303–E322. <https://doi.org/10.1175/BAMS-D-18-0194.1>
- Kropf CM, Ciullo A, Otth L et al (2022) Uncertainty and sensitivity analysis for probabilistic weather and climate-risk modelling: an implementation in CLIMADA v.3.1.0. *Geosci Model Dev* 15(18):7177–7201. <https://doi.org/10.5194/gmd-15-7177-2022>
- Leckebusch GC, Ulbrich U, Fröhlich L et al (2007) Property loss potentials for European midlatitude storms in a changing climate. *Geophys Res Lett*. <https://doi.org/10.1029/2006GL027663>
- Lin X, Kwon WJ (2020) Application of parametric insurance in principle-compliant and innovative ways. *Risk Manag Insur Rev* 23(2):121–150. <https://doi.org/10.1111/rmir.12146>
- Lüthi S, Aznar-Siguan G, Fairless C et al (2021) Globally consistent assessment of economic impacts of wildfires in CLIMADA v.2.2. *Geosci Model Dev* 14(11):7175–7187. <https://doi.org/10.5194/gmd-14-7175-2021>
- Meiler S, Vogt T, Bloemendaal N et al (2022) Intercomparison of regional loss estimates from global synthetic tropical cyclone models. *Nat Commun* 13(1):6156. <https://doi.org/10.1038/s41467-022-33918-1>
- Mitchell-Wallace K, Jones M, Hillier J et al (2017) Natural catastrophe risk management and modelling: a practitioner's guide. Wiley, Hoboken
- Mühlhofer E, Koks EE, Kropf CM et al (2023a) A generalized natural hazard risk modelling framework for infrastructure failure cascades. *Reliab Eng Syst Saf* 234:109194. <https://doi.org/10.1016/j.res.2023.109194>
- Mühlhofer E, Kropf CM, Bresch DN, et al. (2023b) OpenStreetMap for Multi-Faceted Climate Risk Assessments (under review). *Environ Res Commun*. <https://doi.org/10.31223/X5SQ2J>
- Mühlhofer E, Stalhandske Z., Sarcinella M., et al. (2023c) Supporting robust and climate-sensitive adaptation strategies for infrastructure networks: a multi-hazard case study on Mozambique's health-care sector. In: 14th International conference on applications of statistics and probability in civil engineering, ICASP14
- OpenStreetMap contributors (2017) Planet dump retrieved from <https://planet.osm.org>. <https://www.openstreetmap.org>
- Priestley MDK, Pinto JG, Dacre HF et al (2017) The role of cyclone clustering during the stormy winter of 2013/2014. *Weather* 72(7):187–192. <https://doi.org/10.1002/wea.3025>
- Rana A, Zhu Q, Detken A et al (2022) Strengthening climate-resilient development and transformation in Vietnam. *Clim Change* 170(1):4. <https://doi.org/10.1007/s10584-021-03290-y>
- Schwierz C, Köllner-Heck P, Zenklusen Mutter E et al (2010) Modelling European winter wind storm losses in current and future climate. *Clim Change* 101(3):485–514. <https://doi.org/10.1007/s10584-009-9712-1>
- Seity Y, Brousseau P, Malardel S et al (2011) The AROME-France convective-scale operational model. *Mon Weather Rev* 139(3):976–991. <https://doi.org/10.1175/2010MWR3425.1>
- Severino LG, Kropf CM, Afargan-Gerstman H, et al. (2023) Projections and uncertainties of future winter windstorm damage in Europe (under review). *EGU sphere* pp 1–31
- Simpson RH, Saffir H (1974) The Hurricane Disaster-Potential Scale. *Weatherwise* 27(4):169–186. <https://doi.org/10.1080/00431672.1974.9931702>
- Stalhandske Z, Steinmann CB, Meiler S, et al. (2023) Global multi-hazard risk assessment in a changing climate (under review). *Scientific Reports* <https://doi.org/10.31223/X56W9N>
- Stanton EA, Ackerman F, Kartha S (2009) Inside the integrated assessment models: four issues in climate economics. *Clim Dev* 1(2):166–184. <https://doi.org/10.3763/cdev.2009.0015>
- UNDP (2019) Mozambique cyclone Idai post-disaster needs assessment - full report. Tech. rep
- Van Nostrand JM, Nevius JG (2011) Parametric insurance: using objective measures to address the impacts of natural disasters and climate change. *Environ Claims J* 23(3–4):227–237. <https://doi.org/10.1080/10406026.2011.607066>
- Ward PJ, Blauhut V, Bloemendaal N et al (2020) Review article: natural hazard risk assessments at the global scale. *Nat Hazards Earth Syst Sci* 20(4):1069–1096. <https://doi.org/10.5194/nhess-20-1069-2020>
- Welker C, Rössli T, Bresch D (2021) Comparing an insurer's perspective on building damages with modelled damages from pan-European winter windstorm event sets: a case study from Zurich, Switzerland. *Nat Hazard Earth Syst Sci* 21:279–299. <https://doi.org/10.5194/nhess-21-279-2021>
- Zhang J, Tan KS, Weng C (2019) Index insurance design. *ASTIN Bull* 49(2):491–523. <https://doi.org/10.1017/asb.2019.5>